UCLA
UCLA Previously Published Works

Title

Expanding the clinical phenotype in patients with disease causing variants associated with atypical Usher syndrome

Permalink

https://escholarship.org/uc/item/0vc5m5k3

Journal

Ophthalmic Genetics, 42(6)

ISSN

1381-6810

Authors

Igelman, Austin D
Ku, Cristy
da Palma, Mariana Matioli
et al.

Publication Date

2021-11-02

DOI

10.1080/13816810.2021.1946704

Peer reviewed

eScholarship.org Powered by the California Digital Library
University of California

Author Manuscript

Author Manuscript

Author Manuscript

Author Manuscript

HHS Public Access

Author manuscript

Ophthalmic Genet. Author manuscript; available in PMC 2022 December 01.

Published in final edited form as:

Ophthalmic Genet. 2021 December ; 42(6): 664–673. doi:10.1080/13816810.2021.1946704.

Expanding the clinical phenotype in patients with disease causing variants associated with atypical Usher syndrome

Austin D. Igelman, BS[1],

Cristy Ku, MD, PhD[1],

Mariana Matioli da Palma, MD[1,2],

Michalis Georgiou, MD, PhD[3,4],

Elena R. Schiff, PhD[3,4],

Byron L. Lam, MD[5],

Eeva-Marja Sankila, MD[6],

Jeeyun Ahn, MD, PhD[7,8],

Lindsey Pyers, COA[7],

Ajoy Vincent, MBBS, MS[9,10],

Juliana Maria Ferraz Sallum, MD, PhD[2],

Wadih M. Zein, MD[11],

Jin Kyun, Oh BA[12,13],

Ramiro S. Maldonado, MD[14],

Joseph Ryu, BA[12],

Stephen H. Tsang, MD, PhD[12,15],

Michael B. Gorin, MD, PhD[7,16],

Andrew R. Webster, MD(Res), FRCOphth[3,4],

Michel Michaelides, MD(Res), FRCOphth[3,4],

Paul Yang, MD, PhD[1],

Mark E. Pennesi, MD, PhD[1]

[1]-Casey Eye Institute, Oregon Health & Science University, Portland, OR, USA

[2]-Department of Ophthalmology and Visual Sciences, Federal University of São Paulo (UNIFESP), São Paulo, SP, Brazil

[3]-UCL Institute of Ophthalmology, University College London, 11-43 Bath Street, London, EC1V 9EL, UK

[4]-Moorfields Eye Hospital NHS Foundation Trust, City Road, London, EC1V 2PD, UK

[5]-Bascom Palmer Eye Institute, University of Miami Miller School of Medicine, Miami, FL, USA

[6]-Helsinki University Eye Hospital, Helsinki, Finland

Corresponding Author Mark E. Pennesi, MD/PhD, Casey Eye Institute, Oregon Health & Science University, 515 SW Campus Dr. Portland, OR, 97239, USA.

Disclosure of interest: The authors report no conflict of interest.

Author Manuscript Author Manuscript Author Manuscript Author Manuscript

[7]-UCLA Stein Eye Institute, Division of Retinal Disorders and Ophthalmic Genetics, Department of Ophthalmology, David Geffen School of Medicine, UCLA, Los Angeles, CA, USA

[8]-Department of Ophthalmology, Seoul National University, College of Medicine, Seoul Metropolitan Government Seoul National University Boramae Medical Center, Seoul, Korea

[9]-Department of Ophthalmology and Vision Sciences, The Hospital for Sick Children, University of Toronto, Canada.

[10]-Genetics and Genome Biology, The Hospital for Sick Children, Toronto, Canada

[11]-Ophthalmic Genetics and Visual Function Branch, National Eye Institute, National Institutes of Health, Bethesda, MD, USA

[12]-Jonas Children's Vision Care, Departments of Ophthalmology, Pathology & Cell Biology, Columbia Stem Cell Initiative, New York, NY, USA

[13]-State University of New York at Downstate Medical Center, Brooklyn, NY, USA

[14]-University of Kentucky, Department of Ophthalmology and Visual Sciences, Lexington, KY, USA

[15]-Department of Pathology & Cell Biology, Columbia University Irving Medical Center, New York, NY, USA

[16]-Department of Human Genetics, David Geffen School of Medicine, UCLA, Los Angeles, CA, USA

Abstract

Background: Atypical Usher syndrome (USH) is poorly defined with a broad clinical spectrum. Here we characterize the clinical phenotypic of disease caused by variants in *CEP78*, *CEP250*, *ARSG*, and *ABHD12*.

Materials and Methods: Chart review evaluating demographic, clinical, imaging, and genetic findings of 19 patients from 18 families with a clinical diagnosis of retinal disease and confirmed disease causing variants in *CEP78*, *CEP250*, *ARSG*, or *ABHD12*.

Results: *CEP78*-related disease included sensorineural hearing loss (SNHL) in 6/7 patients and demonstrated a broad phenotypic spectrum including: vascular attenuation, pallor of the optic disc, intraretinal pigment, retinal pigment epithelium mottling, areas of mid-peripheral hypo-autofluorescence, outer retinal atrophy, mild pigmentary changes in the macula, foveal hypo-autofluorescence, and granularity of the ellipsoid zone. Nonsense and frameshift variants in *CEP250* showed mild retinal disease with progressive, non-congenital SNHL. *ARSG* variants resulted in a characteristic pericentral pattern of hypo-autofluorescence with one patient reporting non-congenital SNHL. *ABHD12* related disease showed rod-cone dystrophy with macular involvement, early and severe decreased best corrected visual acuity, and non-congenital SNHL ranging from unreported to severe.

Conclusions: This study serves to expand the clinical phenotypes of atypical USH. Given the variable findings, atypical USH should be considered in patients with peripheral and macular retinal disease even without the typical RP phenotype especially when SNHL is noted.

Author Manuscript Author Manuscript Author Manuscript Author Manuscript

Additionally, genetic screening may be useful in patients that have clinical symptoms and retinal findings even in the absence of known SNHL given the variability of atypical USH.

Keywords

Atypical Usher syndrome; CEP78; CEP250; ARSG; ABHD12

Introduction

Usher Syndrome (USH) is an autosomal recessively inherited condition that is the leading cause of deaf-blindness with a prevalence ranging from 1 to 4 people per 25,000 (1). USH is classically characterized by congenital sensorineural hearing loss (SNHL), retinitis pigmentosa (RP), and sometimes vestibular dysfunction. USH is further divided into three types depending on the severity and the age of onset of auditory congenital vestibular dysfunction. USH Type 2 (USH2) generally has an onset of and visual pathology. USH Type 1 (USH1) is the most severe with an onset of RP within the first decade of life, severe congenital SNHL requiring a cochlear implant, and frequently with concomitant RP in the second decade of life and moderate to severe congenital SNHL without vestibular dysfunction. USH Type 3 (USH3) presents with later onset RP, progressive SNHL, and variable vestibular dysfunction. Atypical USH is a poorly defined with significant overlap with other conditions such PHARC (polyneuropathy, hearing loss, ataxia, retinitis pigmentosa, early-onset cataract) and is described as an USH-like phenotype that does not directly fit into either the USH1, USH2, or USH3 phenotypes with a high variability including cases without congenital SNHL, variable relative effects on cones vs rods, and presence of macular disease (2–5).

MYO7A and *CHD23* are the most common genes responsible for USH1 accounting for 70–80% of cases (6). USH2 is known to be caused by variants in several genes including *USH2A*, *GPR98*, and *WHRN* with variants in *USH2A* accounting for 79% of families with USH2 (7–10). USH3 is often associated with variants in the *CLRN1* and *HARS* genes (11–13). *MYO7A*, while commonly associated with USH1, has been reported to cause nonsyndromic recessive deafness, nonsyndromic dominant deafness, and atypical USH (1). Additionally, variants in *USH2A* have been shown to cause non-syndromic RP. It is unclear whether these patients will develop SNHL later in life leading to an atypical USH phenotype (14).

Centrosomal protein 78 (*CEP78*), Centrosomal protein 250 (*CEP250*), arylsulfatase G (*ARSG*), and α/β-hydrolase domain containing 12 (*ABHD12*) have been previously reported as causal for atypical USH (2, 4, 15–25). *CEP78* and *CEP250* are ciliary proteins important for the Usher protein network in retinal photoreceptor cells; *CEP78* acts in ciliogenesis and *CEP250* is expressed on cilia and interacts with *CEP78* (4, 16–22). Separate from the cilia are *ARSG* and *ABHD12*. *ARSG* encodes a sulfatase enzyme and contains a highly conserved catalytic site (15). Only two variants in *ARSG* in six patients have been associated with atypical USH in the literature (23, 26). *ABHD12* encodes a membrane-embedded serine hydrolase that hydrolyzes oxidized phosphatidylserine which is produced in inflammatory conditions and functions as a major lysophosphatidylserine (LPS) lipase in

Author Manuscript Author Manuscript Author Manuscript Author Manuscript

the nervous system (27). Here we describe the clinical, imaging, and genetic findings in 19 patients in 18 families with bi-allelic variants in *CEP78*, *CEP250*, *ASRG*, and *ABHD12* to help characterize these rare conditions.

Materials and Methods

This retrospective multicenter study was conducted at the Casey Eye Institute (CEI) and included cases from CEI, Bascom Palmer Eye Institute (BPEI), Moorfields Eye Hospital (MEH), Helsinki University Eye Hospital (HUEH), University of California at Los Angeles (UCLA), Hospital for Sick Children (HSC), Federal University of Sao Paulo (UNIFESP), the National Eye Institute (NEI), Columbia University Medical Center (CUMC), and the University of Kentucky (UK). This study was approved by the Institutional Review Board of Oregon Health & Science University and met the tenets of the Declaration of Helsinki.

Case Identification

Given the poorly defined nature of atypical USH, the significant overlap with other conditions, and the aim of this paper to move away from a clinical diagnosis and towards a genetic diagnosis, the following inclusion and exclusion criteria were used to query institutional databases for cases. Cases with two known variants in a gene of interest (*CEP78*, *CEP250*, *ARSG*, or *ABHD12*) and retinal disease with or without known SNHL including but not limited to cone-rod dystrophy, rod-cone dystrophy, cone dystrophy, and rod dystrophy were included. Cases that had a clinical phenotype consistent with either USH1, USH2, or USH3 were excluded. The authors reviewed the records of the select patients from their respective institutions and shared data including genetic testing results, demographics, presence and description of possible known consanguinity, presence or absence of SNHL and/or vestibular disease, best corrected visual acuity (BCVA), visual symptoms (e.g. nyctalopia, photophobia), fundoscopic description, and full-field electroretinogram (ffERG). Deidentified color fundus photos, fundus autofluorescence (FAF), ocular coherence tomography (OCT), and kinetic visual fields (KVF) were reviewed, when available, at a single center by the authors at CEI.

Image assessment

Authors at CEI (ADI, CK, MMP, PY, MEP) evaluated color fundus photos, FAF, and OCT images and described the findings. Images from 38 eyes from 19 patients including 12 females (63%) were reviewed in this study for detailed phenotyping. Due to the multi-institutional and retrospective nature of the study, the availability, instrument model, and quality of images varied between cases.

Genetic testing

Genetic testing was performed via a variety of laboratories and specific variant data were collected. Nucleotide and protein changes were reported as recommended by the Human Genome Variation Society. Variations were searched in ClinVar, Varsome, and PubMed. Varsome was used to determine intronic location. The genotype of CEP78–5 was previously evaluated and reported by Sanchis-Juan et al (28).

Author Manuscript Author Manuscript Author Manuscript Author Manuscript

Results

Demographic, ophthalmic, clinical, and genetic features are summarized in Table 1.

CEP78

The age of onset of the six individuals with *CEP78* variants ranged from 11 to 46 years. BCVA at the most recent visit ranged from 20/40 to HM. Patients with longitudinal BCVA data included CEP78–2, CEP78–3, CEP78–5, and CEP78–7 and all but CEP78–2 had progressive worsening of BCVA although CEP78–2 was only seen over 1 year. Two patients (CEP78–18807, CEP78–4) had a cataract noted and two had macular atrophy noted on fundoscopy (CEP78–2, CEP78–4). All but one (CEP78–7) patient had SNHL and one patient (CEP78–18807) had vestibular symptoms. The ffERG of CEP78–87042 had severe rod dysfunction and moderate cone dysfunction although both were abnormal; clinically, they had photophobia and denied nyctalopia. All other patients with reported ffERG results (CEP78–7, CEP78–5, CEP78–4) had cone dysfunction greater than rod dysfunction. Both CEP78–4 and CEP78–5 had a severe rod-cone dystrophy whereas CEP78–7 had a severe cone dystrophy. All reported ffERGs showed cone dysfunction and all of these patients also presented with blurred vision. There was no correlation to ffERG findings and the presence or absence of SNHL. KVF was available only for CEP78–18807 and showed an approximately 40-degree ring scotoma with foveal sparing of the central 10 degrees to a III 4e target along the horizontal meridian for both eyes.

Figure 1 shows representative images of all patients with *CEP78* variants. Imaging of the *CEP78* patients revealed a broad phenotypic spectrum. Color fundus findings included intraretinal pigment, vascular attenuation, pallor of the optic disc, and RPE mottling. FAF showed areas of mid peripheral hypo-autofluorescence ranging from mild to severe with some small zones of macular and foveal hypo-autofluorescence. OCT revealed outer retinal atrophy including granularity of the ellipsoid zone (EZ) (seen in CEP-87042 and CEP78–7) and a spectrum of ONL thinning that spared the fovea until severe disease as illustrated by CEP78–5. Overall, these findings show peripheral greater than central degeneration.

CEP78–87042 and CEP78–7 had biallelic missense variants while all other patients had at most one missense variant. Four of seven patients had homozygous or compound heterozygous variants that likely led to protein truncation of both alleles (CEP78–18807, CEP78–3, CEP78–4, CEP78–5). All intronic variants were canonical splice variants.

CEP250

Age of onset ranged from 13 to 30 years. BCVA at the most recent visit ranged from 20/60 to 20/200. All patients demonstrated progressive SNHL with an age of onset from <10 to 24 years. There were no reports of vestibular symptoms. CEP250–2 and CEP250–3 are siblings with the same homozygous variant. ffERG was obtained on one of the three patients (CEP250–1) which showed a mild cone dystrophy with normal rod function (table 1). KVF was available for CEP250–2 and CEP250–3 which showed fields to approximately 100 degrees along the horizontal meridian to a V 4e target in both eyes. CEP250–3 showed

Author Manuscript Author Manuscript Author Manuscript Author Manuscript

constricted fields to approximately 20 degrees along the horizontal meridian to a V 4e target in both eyes.

Representative images of patients with *CEP250* variants are shown in figure 2. Color fundus analysis revealed normal findings in all patients. FAF demonstrated areas of subtle hyper-autofluorescence in the periphery (CEP250–1) and in the peripapillary region (CEP250–3). CEP250–2 had normal FAF findings. OCT findings showed outer retinal atrophy in all three patients including thinning of the outer nuclear layer (ONL) (CEP250–1) and subtle disruption of the EZ and interdigitation zone (IZ) (CEP250–3).

All variations in *CEP250* were novel and all were nonsense or frameshift variants.

ARSG

Ophthalmologic evaluations of the three patients with *ARSG* variants are summarized in table 1. The age of onset ranged from early 30s to 65 years. ARSG-1 did not have documented SNHL while ARSG-2 and ARSG-29692 had SNHL noted at 50 years old. BCVA at the most recent visit ranged from ARSG-1 reporting BCVA of 20/20 in the right eye and 20/25 in the left to ARSG-29692 with a BCVA at the of 20/800 in her right eye and 20/1000 in her left. Longitudinal BCVA data was only available for ARSG-1 and showed mild relative stability from 20/20 in both eyes to 20/20 in the right eye and 20/25 in the left eye over 8 years. Macular atrophy was noted on fundoscopy in ARSG-2 and ARSG-29692 with the atrophy in ARSG-2 reported to be foveal sparing. ffERG was obtained on one of the three patients (ARSG-2) which showed a moderate rod-cone dystrophy (table 1). KVF was available only for ARSG-29692 which showed a central scotoma to approximately 75 degrees along the horizontal meridian to a III 4e target in both eyes.

Representative from these patients are shown in figure 3. Color fundus analysis showed parafoveal and mid-peripheral RPE atrophy, optic disc pallor, and intraretinal pigment. FAF of all patients demonstrated near mid-peripheral and pericentral hypo-autofluorescence. Additionally, ARSG-29692 showed advanced disease and severe macular involvement with central hypo-autofluorescence, ARSG-2 displayed milder macular involvement including a hypo-autofluorescent parafoveal ring, and ARSG-1 demonstrated foveal sparing disease and a parafoveal hyper-autofluorescent ring. This range was highlighted in OCT with extensive outer retinal atrophy affecting the fovea in ARSG-29692, whereas ARSG-1 and ARSG-2 showed foveal sparing atrophy.

The patient with the most severe disease, ARSG-29692, had homozygous missense variants while the other two patients had one missense variant and either one intronic splice site (ARSG-1) or frame shift (ARSG-2) variant.

ABHD12

Age of onset of the six patients with *ABHD12* disease ranged from 16 years to early the 30s. Four presented with central blurring. None reported vestibular dysfunction and three had progressive SNHL with an age of onset ranging from 20–44 years. Of the four patients with longitudinal BCVA data, all but one (ABHD12–2) had progressive worsening. Four patients had BCVA of 20/200 or worse in both eyes. While these patients had severely decreased

Author Manuscript Author Manuscript Author Manuscript Author Manuscript

BCVA at an early age, ABHD12–1 showed 20/25 BCVA at age 48 years. ffERG was obtained on four patients; three (ABHD12–2, ABHD12–3, ABHD12–4) were suggestive of rod-cone dystrophy and one (ABHD12–1) was undetectable for both rods and cones. All three patients with a rod-cone dystrophy had mild cone dysfunction but rod dysfunction included mild (ABHD12–3), moderate (ABHD12–4), and severe (ABHD12–2). KVF was obtained only on ABHD12–1 and showed constricted visual fields to 50 degrees with a central scotoma of 10 degrees along the horizontal meridian to a V 4e target.

All patients with *ABHD12* variants showed macular findings with fundoscopy revealing atrophy of the macula in four patients. Additionally, color fundus showed macular changes in all patients ranging from mild granular changes in ABHD12–2 to significant RPE atrophy in ABHD12–6. Color fundus photos also showed a variety of changes including vascular attenuation (ABHD12–1, ABHD12–4, ABHD12–5, ABHD12–6) and intraretinal pigment (ABHD12–1, ABHD12–5, ABHD12–6). FAF revealed a range of phenotypes; however, all images revealed macular involvement ranging from central hypo-autofluorescence (ABHD12–3, ABHD12–4) to severe global hypo-autofluorescence (ABHD12–6). OCT revealed fovea-involving outer retinal atrophy in all patients as well as sub-retinal deposits in four patients (ABHD12–1, ABHD12–2, ABHD12–3, ABHD12–4). Figure 4 shows color fundus photos, FAF, and OCT images of each affected patient.

ABHD12–3 was homozygous for a truncating variant and ABHD12–4 and ABHD12–6 had homozygous or compound heterozygous variants that likely lead to protein truncation on both alleles. All intronic variants were splicing variants. None of the patients in this study had ataxia noted however no formal evaluation was conducted.

Discussion

While USH1, USH2, and USH3 are well categorized, atypical USH is inherently a group of highly variable conditions that are primarily defined by their divergence from the three major subcategories of USH. The clinical phenotypes associated with *CEP78, CEP250, ARSG,* and *ABHD12* are not well characterized (4, 21, 23, 25, 26).

CEP78 is a ciliary/centrosomal protein present in both the inner ear and retina. In the retina, it is localized to the base of the photoreceptor connecting cilium particularly in cone photoreceptors (2, 21). Two of our reported missense variants (p.Leu108Trp and p.Ser147Leu) are predicted to disrupt the leucine rich repeat motif (LRR) found in the *CEP78* protein. Other variants recorded included two whole deletions, a nonsense, an inversion, two splicing, and one variant after the LRR. While there was no correlation between variants in the LRR and retinal phenotypic subtype, all patients with subtype 2 had biallelic missense variants and none of the patients with subtype 1 had biallelic missense variants suggesting a possible relationship.

Analysis of the patients with *CEP78* related disease showed a preponderance for SNHL with 6/7 patients being affected by their last visit which is consistent with previous reports of CRD with SNHL (20, 21, 28). Most patients affected had an early onset SNHL while only one (CEP78–5) had an onset later than the second decade of life. While CEP78–7 did not

Author Manuscript Author Manuscript Author Manuscript Author Manuscript

have recorded SNHL, it is possible that they have not been tested recently or that it has not yet manifested as they were 25 years old at the last appointment.

Previous reports of *CEP78* related retinal disease often describe a cone rod dystrophy (CRD) phenotype (20, 21). Our patients showed a CRD clinical phenotype similar to previously reported literature and all reported ffERGs besides CEP78–87042 had cone greater than rod dysfunction. Despite this ffERG finding, CEP78–87042 still reported clinical symptoms more associated with a CRD such as photophobia supporting the association of CRD with *CEP78* variants.

The retinal findings show a broad phenotypic spectrum. Some of the reported findings are similar to previous cases of CEP78 related retinal disease described in the literature which have shown disappearance of the ellipsoid zone (EZ) on OCT and mid-peripheral hypo-autofluorescence along the vascular arcades (4, 20). There was a range in severity especially with regards to the hypo-autofluorescence ranging from small, mild areas (CEP78–3) to a confluent ring in the midperiphery (CEP78–5). Other findings were such as the granularity of the EZ were different than the previously reported cases of *CEP78* related retinal disease. This suggests that the phenotypic spectrum of *CEP78* disease is broad and this study serves to broaden our understanding in patients with biallelic missense variants.

Our patients with *CEP250* variants exhibited nonsense and frameshift variants suggesting that this phenotype of mild RP with progressive SNHL may be specific for biallelic *CEP250* nonsense or frameshift variants that lead to defective proteins in the absence of pathogenic variants in other genes. *CEP250* is involved in centrosomal and ciliary function and a knock-in nonsense variant mouse model showed decreased scotopic and photopic ERG responses with a larger decrease in scotopic responses. This mouse study also showed decreased retinal thickness due to changes in the ONL (29).

Kubota et al. reported heterozygous truncating variants (c.361C>T, p.R121* and c.562C>T, p.R188*) in *CEP250* that lead to atypical USH with minimal but present SNHL and RP (25). Another study showed a homozygous nonsense variant in *CEP250* and a single variant in PCARE led to a phenotype that was similar to that described by Kubota et al. and are consistent with our findings which showed FAF ranging from normal to demonstrating areas of mild hyper-autofluorescence, normal color fundus findings, disruption of the IZ and EZ on OCT, and progressive SNHL by their mid 20s.

Three patients had *ARSG* variants in this study. Imaging from all patients showed a pericentral pattern of hypo-autofluorescence highly characteristic of previous reports (23, 26). Similar to other studies, there may be progressive macular involvement with initial foveal sparing progressing to severe outer retinal atrophy involving the entire macula as in ARSG-29692 (23). Moderate to severe SNHL has also been reported in the literature corroborating the severe SNHL in ARSG-29692 and moderate SNHL in ARSG-2. ARSG-1 showed no SNHL, however, they may develop it later in life as both ARSG-2 and ARSG-29692 did not develop SNHL until 50 years old. While the most advanced patient was the only patient with homozygous missense variants, they also presented at the latest

Author Manuscript Author Manuscript Author Manuscript Author Manuscript

age (69 years) making it difficult to ascertain whether the severity is due to specific variants or the age of the patient.

An *ARSG* knockout (KO) mouse model demonstrated significant (ONL) thinning suggesting photoreceptor degeneration. Cone density appeared to be unaffected in this study implying rod specific disease (30). No ERG data was available for our patients to evaluate cone vs rod function. Given that *ARSG* expression appears to be restricted to the murine RPE, it is possible that the photoreceptor degeneration is due to RPE dysfunction although the specific mechanism has not yet been elucidated in this model (30).

Patients with *ABHD12* variants showed early severe decreased BCVA with several patients experiencing 20/200 BCVA or worse in their third or fourth decade of life similar to a previous report (31). Additionally, macular atrophy was common and FAF often showed atrophic areas of hypo-autofluorescence. Some patients showed parafoveal hyper-autofluorescence indicating injured RPE which has been reported before in *ABHD12* disease (32). Severe macular findings on FAF and OCT including outer retinal atrophy and sub-retinal deposits largely correspond to the severity of BCVA loss. Specifically, ABHD12–5 and ABHD12–1 showed significant FAF changes and reported BCVAs of HM and LP respectively. These findings suggest that *ABHD12* related disease may be more severe than that caused by variants in *CEP78*, *CEP250*, and *ARSG*.

ABHD12 variants have been implicated in PHARC (polyneuropathy, hearing loss, ataxia, retinitis pigmentosa, early-onset cataract) and a KO *ABHD12* mouse model has led to a PHARC-like phenotype (31, 33–35). This mouse model suggests that *ABHD12* dysfunction leads to changes in LPS metabolism resulting in elevated levels of proinflammatory lipids and neurologic abnormalities. Cataracts and SNHL were observed in ABHD12–4 and ABHD12–5, however, no formal neurologic assessments were conducted. SNHL was also not reported in three of the six patients. The homozygous variants in ABHD12–3 has been previously reported by Eisenberger et al. in two siblings both with hearing loss noted at age 14 years old, cataract surgery in the third decade of life, retinal changes and BCVA of finger counting by ages 38 and 55 years old (31). One patient reported by Eisenberger et al. had an ataxic gait but no cerebellar atrophy a common finding in PHARC, noted on CT while the sibling had no reported ataxia or balance problems (31). ABHD12–3 has no reported cataract, SNHL, or ataxia. The cataracts in PHARC were reported as posterior subcapsular which are common in RP further suggesting a spectrum rather than distinct conditions (31). There was no noted association between variant type and severity in this study.

Most reports of *ABHD12* related retinal disease diagnose patients with PHARC, although all symptoms are not uniformly present and some consider *ABHD12* a rare USH gene highlighting the heterogeneity of retinal disease and syndromes related to genes indicated in USH (31–34, 36).

Our study highlights that *ABHD12*-related retinal disease, characterized by severe BCVA loss and macular involvement, may be more commonly unassociated with a PHARC diagnosis than previously thought, although long term follow-up would be needed to determine this conclusively.

Author Manuscript Author Manuscript Author Manuscript Author Manuscript

While the retrospective nature and the variation in follow-up, imaging, and other diagnostic testing make the characterizations that can be drawn from this study uncertain, several conclusions are supported by these findings.

The peripheral retina is affected first in typical USH and macular disease leading to decreased BCVA occurs later in the process. Congenital hearing loss is one of the defining features across the typical USH groups. The phenotype of atypical USH, however, is highly variable and our study demonstrated a broad range of retinal phenotypes including some with early macular involvement and others with a more typical RP presentation. Our study included patients with congenital SNHL, non-congenital SNHL, and no reported SNHL at the time of the last visit suggesting that, even within genotypes, the age of onset of SNHL is variable. Given the variable findings described here, atypical USH should be considered in patients with peripheral and/or macular retinal degeneration with late onset SNHL even without the classic RP phenotype. Additionally, genetic screening for atypical USH genes may be useful in patients that have retinal findings and clinical symptoms even without documented SNHL given the variability of expression. Patients with rare conditions such as atypical USH can often be misdiagnosed with more common conditions such as non-syndromic RP. While there are currently no approved treatments for atypical USH, genetic testing is crucial to give patients and clinicians a better understanding of prognosis and is almost always required for enrollment in future clinical trials.

Acknowledgements

The authors would like to thank Delphine Blain, ScM, MBA - Certified Genetic Counselor for support with this project.

Funding: This work is funded by the National Institutes of Health [P30EY010572, K08EY026650, 5P30CA013696, U01EY030580, U54OD020351, R24EY028758, R01EY009076, R24EY027285, 5P30EY019007, R01EY018213, R01EY024698, R01EY024091, R01EY026682, R21AG050437NIH intramural research fund], the Research to Prevent Blindness [unrestricted grant for Casey Eye Institute, unrestricted grant for UCLA], the Foundation Fighting Blindness [CD-NMT-0714-0648, CD-CL-0617-0727-HSC], New York Regional Research Center Grant [PPA-1218-0751-COLU], Jonas Children's Vision Care and Bernard & Shirlee Brown Glaucoma Laboratory, the Schneeweiss Stem Cell Fund, New York State [SDHDOH01-C32590GG-3450000], Nancy & Kobi Karp, the Crowley Family Funds, the Rosenbaum Family Foundation, Alcon Research Institute, and the Gebroe Family Foundation, Harold and Pauline Price Foundation, Nina Abrams Fund, ames V. Bastek, M.D. Hereditary Retinal Disease Research Program, the Coordenação de Aperfeiçoamento de Pessoal de Nível Superior - Brasil (CAPES) - Finance Code 001, and the National Institute for Health Research Biomedical Research Centre at Moorfields Eye Hospital NHS Foundation Trust and UCL Institute of Ophthalmology. The sponsors or funding organizations had no role in the design or conduct of this research.

References

1. Mathur P, Yang J. Usher syndrome: Hearing loss, retinal degeneration and associated abnormalities. Biochim Biophys Acta. 2015;1852(3):406–20. [PubMed: 25481835]
2. Nolen RM, Hufnagel RB, Friedman TB, Turriff AE, Brewer CC, Zalewski CK, et al. Atypical and ultra-rare Usher syndrome: a patients with Usher syndrome type 1. J Hum Genet. 2010;55(12):796–800. [PubMed: 20844544]
3. Bashir R, Fatima A, Naz S. A frameshift mutation in SANS results in atypical Usher syndrome. Clin Genet. 2010;78(6):601–3. [PubMed: 21044053]
4. Fu Q, Xu M, Chen X, Sheng X, Yuan Z, Liu Y, et al. CEP78 is mutated in a distinct type of Usher syndrome. J Med Genet. 2017;54(3):190–5. [PubMed: 27627988]

Author Manuscript Author Manuscript Author Manuscript Author Manuscript

5. Liu X-Z, Hope C, Walsh J, Newton V, Ke XM, Liang CY, et al. Mutations in the myosin VIIA gene cause a wide phenotypic spectrum, including atypical Usher syndrome. The American Journal of Human Genetics. 1998;63(3):909–12. [PubMed: 9718356]
6. Nakanishi H, Ohtsubo M, Iwasaki S, Hotta Y, Takizawa Y, Hosono K, et al. Mutation analysis of the MYO7A and CDH23 genes in Japanese review. Ophthalmic Genetics. 2020:1–12.
7. Eudy JD, Weston MD, Yao S, Hoover DM, Rehm HL, Ma-Edmonds M, et al. Mutation of a gene encoding a protein with extracellular matrix motifs in Usher syndrome type IIa. Science. 1998;280(5370):1753–7. [PubMed: 9624053]
8. Weston MD, Luijendijk MW, Humphrey KD, Moller C, Kimberling WJ. Mutations in the VLGR1 gene implicate G-protein signaling in the pathogenesis of Usher syndrome type II. Am J Hum Genet. 2004;74(2):357–66. [PubMed: 14740321]
9. Ebermann I, Scholl HP, Charbel Issa P, Becirovic E, Lamprecht J, Jurklies B, et al. A novel gene for Usher syndrome type 2: mutations in the long isoform of whirlin are associated with retinitis pigmentosa and sensorineural hearing loss. Hum Genet. 2007;121(2):203–11. [PubMed: 17171570]
10. Le Quesne Stabej P, Saihan Z, Rangesh N, Steele-Stallard HB, Ambrose J, Coffey A, et al. Comprehensive sequence analysis of nine Usher syndrome genes in the UK National Collaborative Usher Study. J Med Genet. 2012;49(1):27–36. [PubMed: 22135276]
11. Fields RR, Zhou G, Huang D, Davis JR, Möller C, Jacobson SG, et al. Usher syndrome type III: revised genomic structure of the USH3 gene and identification of novel mutations. Am J Hum Genet. 2002;71(3):607–17. [PubMed: 12145752]
12. Joensuu T, Hämäläinen R, Yuan B, Johnson C, Tegelberg S, Gasparini P, et al. Mutations in a novel gene with transmembrane domains underlie Usher syndrome type 3. Am J Hum Genet. 2001;69(4):673–84. [PubMed: 11524702]
13. Puffenberger EG, Jinks RN, Sougnez C, Cibulskis K, Willert RA, Achilly NP, et al. Genetic mapping and exome sequencing identify variants associated with five novel diseases. PLoS One. 2012;7(1):e28936-e.
14. Pierrache LH, Hartel BP, van Wijk E, Meester-Smoor MA, Cremers FP, de Baere E, et al. Visual Prognosis in USH2A-Associated Retinitis Pigmentosa Is Worse for Patients with Usher Syndrome Type IIa Than for Those with Nonsyndromic Retinitis Pigmentosa. Ophthalmology. 2016;123(5):1151–60. [PubMed: 26927203]
15. Abitbol M, Thibaud J-L, Olby NJ, Hitte C, Puech J-P, Maurer M, et al. A canine Arylsulfatase G (ARSG) mutation leading to a sulfatase deficiency is associated with neuronal ceroid lipofuscinosis. Proc Natl Acad Sci U S A. 2010;107(33):14775–80. [PubMed: 20679209]
16. Brunk K, Zhu M, Barenz F, Kratz AS, Haselmann-Weiss U, Antony C, et al. Cep78 is a new centriolar protein involved in Plk4-induced centriole overduplication. J Cell Sci. 2016;129(14):2713–8. [PubMed: 27246242]
17. Fogeron ML, Muller H, Schade S, Dreher F, Lehmann V, Kuhnel A, et al. LGALS3BP regulates centriole biogenesis and centrosome hypertrophy in cancer cells. Nat Commun. 2013;4:1531. [PubMed: 23443559]
18. Fry AM, Mayor T, Meraldi P, Stierhof YD, Tanaka K, Nigg EA. C-Nap1, a novel centrosomal coiled-coil protein and candidate substrate of the cell cycle-regulated protein kinase Nek2. J Cell Biol. 1998;141(7):1563–74. [PubMed: 9647649]
19. Maerker T, van Wijk E, Overlack N, Kersten FF, McGee J, Goldmann T, et al. A novel Usher protein network at the periciliary reloading point between molecular transport machineries in vertebrate photoreceptor cells. Hum Mol Genet. 2008;17(1):71–86. [PubMed: 17906286]
20. Namburi P, Ratnapriya R, Khateb S, Lazar CH, Kinarty Y, Obolensky A, et al. Bi-allelic Truncating Mutations in CEP78, Encoding Centrosomal Protein 78, Cause Cone-Rod Degeneration with Sensorineural Hearing Loss. Am J Hum Genet. 2016;99(3):777–84. [PubMed: 27588452]
21. Nikopoulos K, Farinelli P, Giangreco B, Tsika C, Royer-Bertrand B, Mbefo MK, et al. Mutations in CEP78 Cause Cone-Rod Dystrophy and Hearing Loss Associated with Primary-Cilia Defects. Am J Hum Genet. 2016;99(3):770–6. [PubMed: 27588451]

Author Manuscript Author Manuscript Author Manuscript Author Manuscript

22. Sorusch N, Wunderlich K, Bauss K, Nagel-Wolfrum K, Wolfrum U. Usher syndrome protein network functions in the retina and their relation to other retinal ciliopathies. Adv Exp Med Biol. 2014;801:527–33. [PubMed: 24664740]

23. Khateb S, Kowalewski B, Bedoni N, Damme M, Pollack N, Saada A, et al. A homozygous founder missense variant in arylsulfatase G abolishes its enzymatic activity causing atypical Usher syndrome in humans. Genet Med. 2018;20(9):1004–12. [PubMed: 29300381]

24. Khateb S, Zelinger L, Mizrahi-Meissonnier L, Ayuso C, Koenekoop RK, Laxer U, et al. A homozygous nonsense CEP250 mutation combined with a heterozygous nonsense C2orf71 mutation is associated with atypical Usher syndrome. J Med Genet. 2014;51(7):460–9. [PubMed: 24780881]

25. Kubota D, Gocho K, Kikuchi S, Akeo K, Miura M, Yamaki K, et al. CEP250 mutations associated with mild cone-rod dystrophy and sensorineural hearing loss in a Japanese family. Ophthalmic Genet. 2018;39(4):500–7. [PubMed: 29718797]

26. Abad-Morales V, Navarro R, Burés-Jelstrup A, Pomares E. Identification of a novel homozygous ARSG mutation as the second cause of Usher syndrome type 4. Am J Ophthalmol Case Rep. 2020;19:100736-.

27. Kelkar DS, Ravikumar G, Mehendale N, Singh S, Joshi A, Sharma AK, et al. A chemical-genetic screen identifies ABHD12 as an oxidized-phosphatidylserine lipase. Nat Chem Biol. 2019;15(2):169–78. [PubMed: 30643283]

28. Sanchis-Juan A, Stephens J, French CE, Gleadall N, Mégy K, Penkett C, et al. Complex structural variants in Mendelian disorders: identification and breakpoint resolution using short- and long-read genome sequencing. Genome Med. 2018;10(1):95-. [PubMed: 30526634]

29. Huang X-F, Xiang L, Fang X-L, Liu W-Q, Zhuang Y-Y, Chen Z-J, et al. Functional characterization of CEP250 variant identified in nonsyndromic retinitis pigmentosa. Human Mutation. 2019;40(8):1039–45. [PubMed: 30998843]

30. Kruszewski K, Lüllmann-Rauch R, Dierks T, Bartsch U, Damme M. Degeneration of Photoreceptor Cells in Arylsulfatase G-Deficient Mice. Investigative Ophthalmology & Visual Science. 2016;57(3):1120–31.

31. Eisenberger T, Slim R, Mansour A, Nauck M, Nürnberg G, Nürnberg P, et al. Targeted next-generation sequencing identifies a homozygous nonsense mutation in ABHD12, the gene underlying PHARC, in a family clinically diagnosed with Usher syndrome type 3. Orphanet J Rare Dis. 2012;7:59. [PubMed: 22938382]

32. Thimm A, Rahal A, Schoen U, Abicht A, Klebe S, Kleinschnitz C, et al. Genotype-phenotype correlation in a novel ABHD12 mutation underlying PHARC syndrome. J Peripher Nerv Syst. 2020;25(2):112–6. [PubMed: 32077159]

33. Li T, Feng Y, Liu Y, He C, Liu J, Chen H, et al. A novel ABHD12 nonsense variant in Usher syndrome type 3 family with genotype-phenotype spectrum review. Gene. 2019;704:113–20. [PubMed: 30974196]

34. Yoshimura H, Hashimoto T, Murata T, Fukushima K, Sugaya A, Nishio SY, et al. Novel ABHD12 mutations in PHARC patients: the differential diagnosis of deaf-blindness. Ann Otol Rhinol Laryngol. 2015;124 Suppl 1:77s–83s. [PubMed: 25743180]

35. Blankman JL, Long JZ, Trauger SA, Siuzdak G, Cravatt BF. ABHD12 controls brain lysophosphatidylserine pathways that are deregulated in a murine model of the neurodegenerative disease PHARC. Proc Natl Acad Sci U S A. 2013;110(4):1500–5. [PubMed: 23297193]

36. Sun T, Xu K, Ren Y, Xie Y, Zhang X, Tian L, et al. Comprehensive Molecular Screening in Chinese Usher Syndrome Patients. Invest Ophthalmol Vis Sci. 2018;59(3):1229–37. [PubMed: 29625443]

Author Manuscript Author Manuscript Author Manuscript Author Manuscript

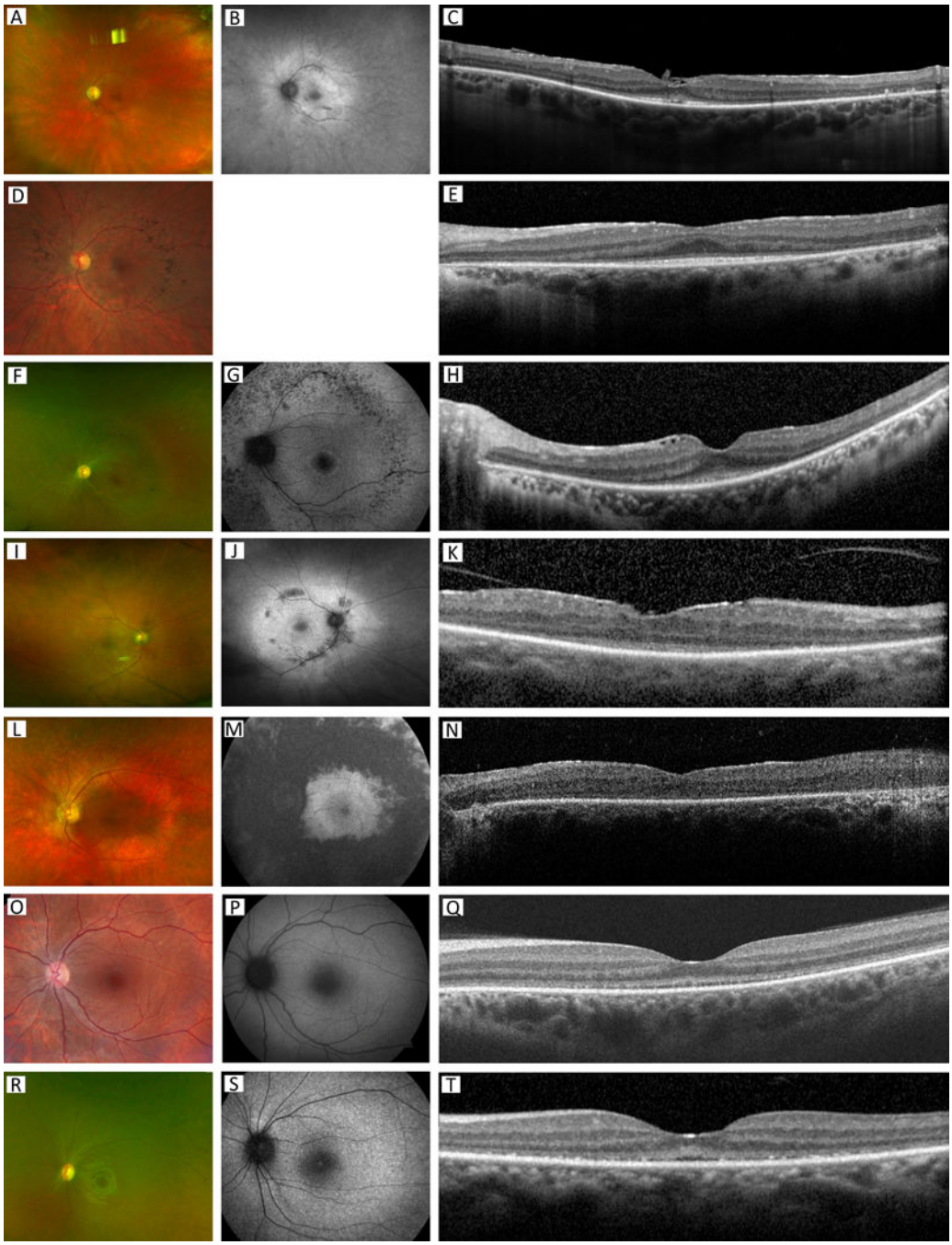

Figure 1: Representative multimodal imaging of patients with *CEP78*-related disease

CEP78–18807 (A – C), CEP78–2 (D, E), CEP78–3 (F – H), CEP78–4 (I – K), CEP78–5 (L – N), CEP78–87042 (O – Q) CEP78–7 (R – T). CFP (A, D, F, I, L, O, R), FAF (B, G, J, M, P, S), OCT sections (C, E, H, K, N, Q, T) demonstrating the spectrum of disease. Subtype 1 depicts an RP like phenotype including vascular attenuation, pallor of the optic disc, and RPE mottling on CFP (A, D, F, I, L), areas of mid peripheral hypo- autofluorescence ranging from mild to severe on FAF (B, G, J, M), and outer retinal atrophy on OCT (C, E, H, K). Common findings in subtype 1 include foveal hypo-autofluorescence (P, S) and

granularity of the ellipsoid zone (Q, T). Abbreviations: CFP, color fundus photos; FAF, fundus auto-fluorescence; OCT, optical coherence tomography; ERM, epiretinal membrane.

Author Manuscript Author Manuscript Author Manuscript Author Manuscript

Author Manuscript Author Manuscript Author Manuscript Author Manuscript

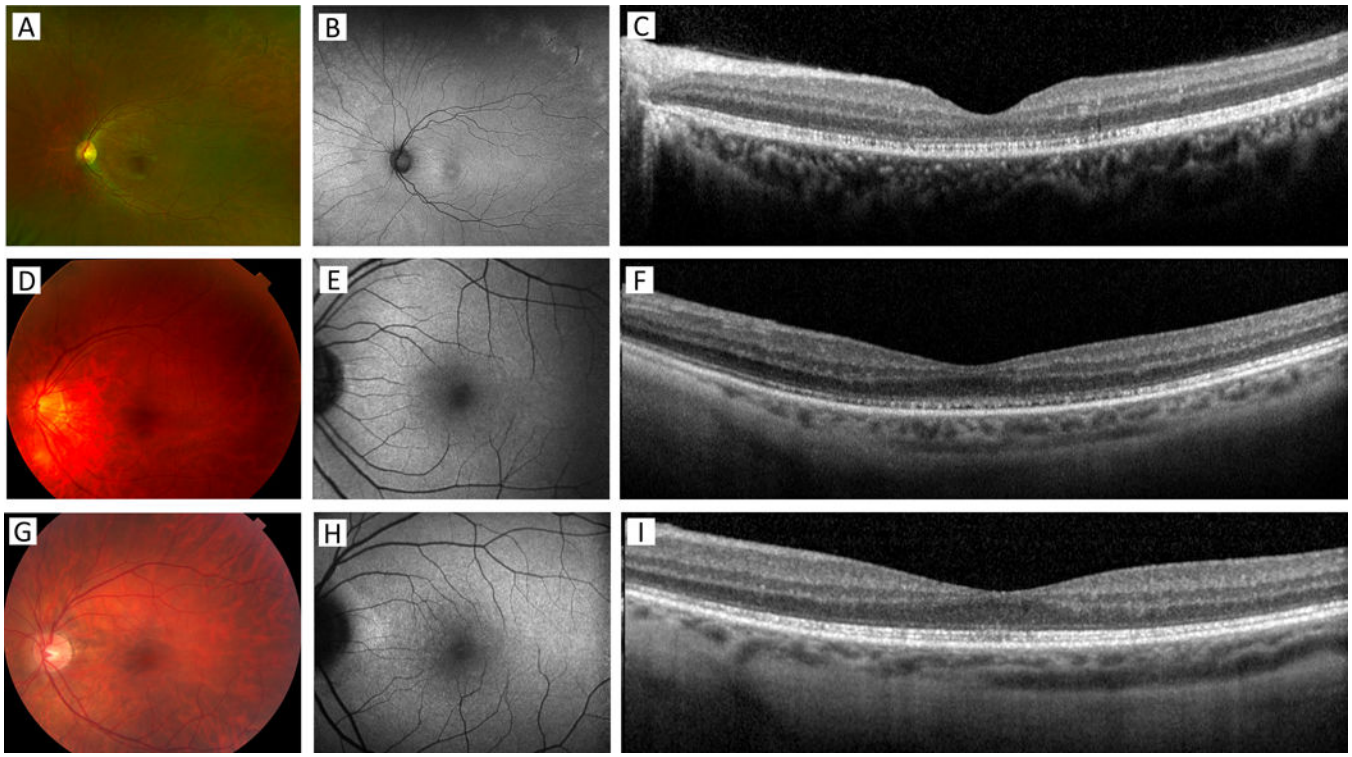

Figure 2: Representative multimodal imaging of patients with *CEP250*-related disease

CEP250–1 (A – C), CEP250–2 (D – F), CEP250–3 (G – I). CFP (A, D, G), FAF (B, E, H), OCT sections (C, F, I) demonstrating the spectrum of disease. CFP revealed normal findings in all patients (A, D, G). FAF ranged from normal (E) to areas of subtle hyper-autofluorescence in the periphery (B) and in the peripapillary region (H). OCT findings showed outer retinal atrophy in all three patients including thinning of the outer nuclear layer (C) and subtle disruption of the ellipsoid zone and interdigitation zone (I). Abbreviations: CFP, color fundus photos; FAF, fundus auto-fluorescence; OCT, optical coherence tomography.

Author Manuscript Author Manuscript Author Manuscript Author Manuscript

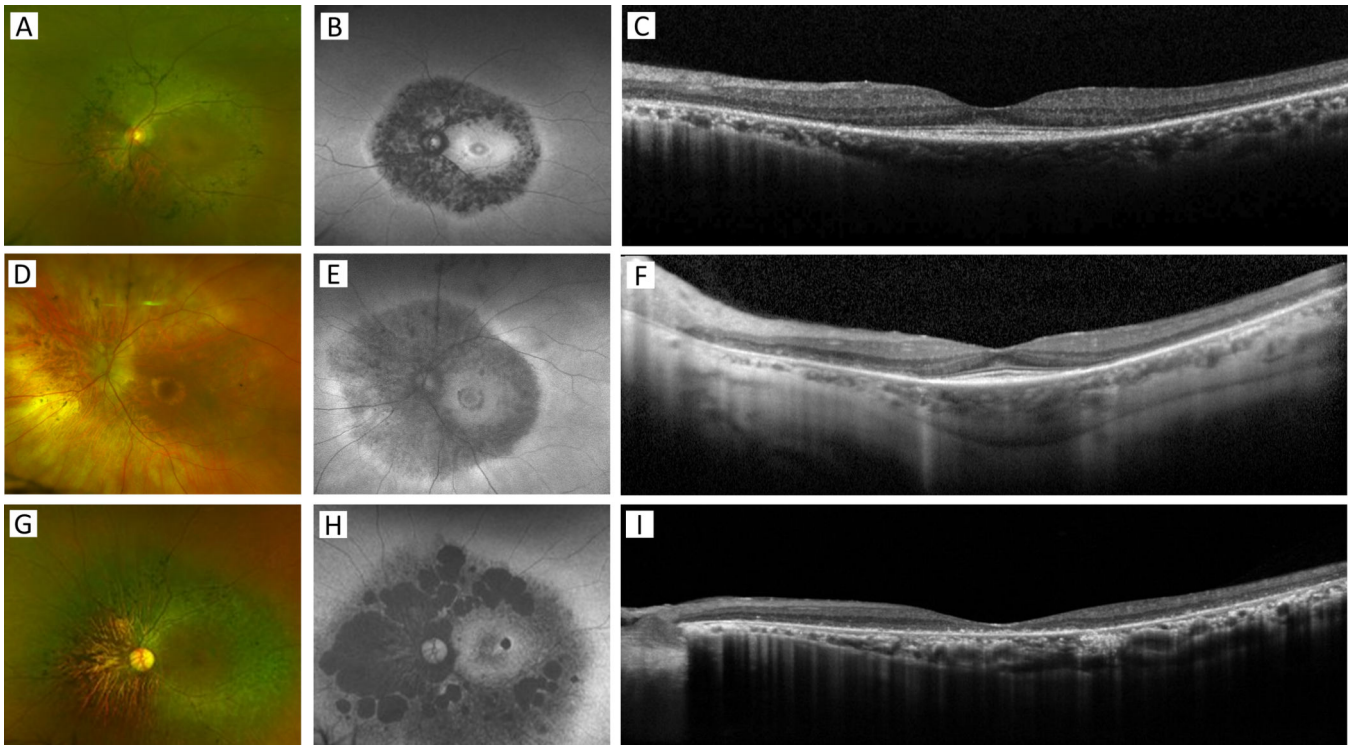

Figure 3: Representative multimodal imaging of patients with *ARSG*-related disease

ARSG-1 (A – C), ARSG-2 (D – F). ARSG-29692 (G – I). CFP (A, D, G), FAF (B, E, H), OCT sections (C, F, I) demonstrating the spectrum of disease. CFP showed parafoveal and mid-peripheral RPE atrophy, intraretinal pigment, and optic disc pallor (A, D, G). FAF of all patients demonstrated pericentral and mid-peripheral hypo-autofluorescence (B, E, H). ARSG-29692 revealed advanced disease and macular involvement with central hypo-autofluorescence (H), ARSG-2 showed a parafoveal ring of hypo-autofluorescence (E), and ARSG-1 demonstrated a parafoveal hyper-autofluorescent ring (B). OCT revealed extensive outer retinal atrophy involving the foveal in ARSG-29692 (I), and foveal sparing atrophy in ARSG-1 and ARSG-2 (C, F). Abbreviations: CFP, color fundus photos; FAF, fundus auto-fluorescence; OCT, optical coherence tomography.

Author Manuscript Author Manuscript Author Manuscript Author Manuscript

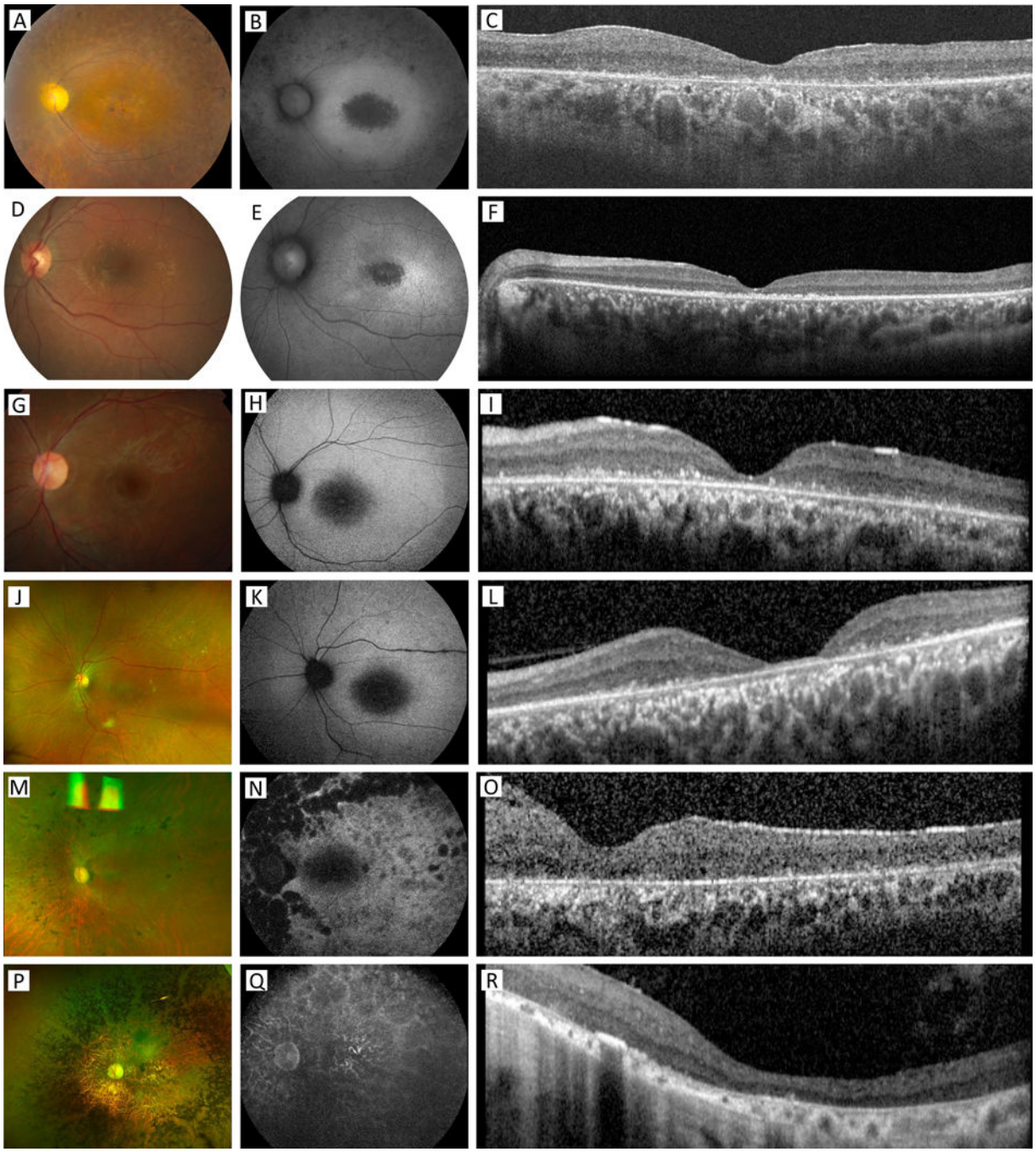

Figure 4: Representative multimodal imaging of patients with *ABHD12*-related disease

ABHD12–1 (A – C), ABHD12–2 (D – F), ABHD12–3 (G – I), ABHD12–4 (J – L), ABHD12–5 (M – O), ABHD12–6 (P – RCFP (A, D, G, J, M, P), FAF (B, E, H, K, N, Q), OCT sections (C, F, I, L, O, R) demonstrating the spectrum of disease. CFP showed macular changes in all patients ranging from mild granular changes (D) to significant RPE atrophy (P). FAF revealed macular involvement ranging from central hypo-autofluorescence (H, K) to severe global hypo-autofluorescence (Q). OCT showed fovea-involving outer retinal

atrophy and as sub-retinal deposits. Abbreviations: CFP, color fundus photos; FAF, fundus auto-fluorescence; OCT, optical coherence tomography.

Author Manuscript Author Manuscript Author Manuscript Author Manuscript

Author Manuscript Author Manuscript Author Manuscript Author Manuscript

Table 1:

Demographic and ophthalmic features of identified cases

ID	Sex	Age ofA Sx onset (y)	Age at 1st visit (y)	BCVA at 1st visit (OD; OS)	Age at last visit (y)	BCVA at last visit (OD; OS)	Presenting ocular Sx	Cataract	Macular findings	ffERG	SNHL onset (y)	Ves. Sx	CS	Allele 1; Allele 2
CEP78														
CEP78–18807	F	35	58	20/40; 20/50	N/A	N/A	Nyctalopia	Yes	RPE mottling	N/A	Mild Progressive (birth)	Yes	No	Whole deletion; c.211delG, p.Val71Serfs*18
CEP78–2	F	18	30	20/40; 20/40	31	20/40; 20/40	Reduced PV	No	Atrophy	N/A	Mod. Progressive (18)	No	No	c.254–1G>T, Intron 1; c.323T>G, p.Leu108Trp
CEP78–3	F	Teens	22	20/16.7; 20/16.7	40	20/100; 20/80	Nyctalopia	No	No	N/A	Mild Unclear Progression (15)	No	Yes	c.1629–7C>A, Intron 13; c.1629–7C>A, Intron 13
CEP78–4	F	40	70	20/800; 20/800	N/A	N/A	Blurred CV	Yes	Atrophy and ERM	Sev. CRD	Mod., Stable (birth)	No	No	c.635G>A, p.Trp212*; Whole deletion
CEP78–5	M	46	46	20/300; 20/400	68	HM; HM	Blurred CV	No	No	Sev. CRD	Progressive (50)	No	Unknown	Inversion der(9)(q21.2); Inversion der(9)(q21.2)
CEP78–87042	F	18	22	20/100; 20/100	N/A	N/A	Blurred CV	No	RPE granularity	Sev. RD, mod. CD	Severe Stable (12)	No	No	c.440C>T, p.Ser147Leu; c.440C>T, p.Ser147Leu
CEP78–7	F	11	20	20/120; 20/120	25	20/125; 20/160	Blurred CV	No	No	Sev. CD	No	No	Yes	c.1175C>T, p.Pro392Leu; c.1175C>T, p.Pro392Leu
CEP250														
CEP250–1	M	<18	25	20/70; 20/70	N/A	N/A	Blurred CV and ICD	No	Atrophy	Mild CD	Mod. Progressive (<10)	No	No	c.2512delC, p.Gln838Lysfs*18; c.5579_5580dupAG, p.Leu1861Serfs*33
CEP250–2 *	F	30	46	20/60; 20/100	N/A	N/A	Blurred CV, glare, nyctalopia	Yes	Punctate yellow deposits	N/A	Severe Progressive (22)	No	No	c. 5959C>T, p.Gln1987*; c. 5959C>T, p.Gln1987*;

Author Manuscript Author Manuscript Author Manuscript Author Manuscript

ID	Sex	Age ofA Sx onset (y)	Age at 1st visit (y)	BCVA at 1st visit (OD; OS)	Age at last visit (y)	BCVA at last visit (OD; OS)	Presenting ocular Sx	Cataract	Macular findings	ffERG	SNHL onset (y)	Ves. Sx	CS	Allele 1; Allele 2
CEP250–3 *	F	13	31	20/160; 20/200	N/A	N/A	Blurred CV, Nyctalopia, reduced PV	Yes	RPE granularity	N/A	Mod. Progressive (24)	No	No	c. 5959C>T, p.Gln1987*; c. 5959C>T, p.Gln1987*
ARSG														
ARSG-1	M	Early 30s	40	20/20; 20/20	48	20/20; 20/25	Nyctalopia, reduced PV and depth perception	Yes	No	N/A	No	No	No	c.283C>T, p.Arg95Trp; c.566+3_566+8del, Intron 5
ARSG-2	F	65	65	20/30; 20/25	N/A	N/A	None	No	Foveal sparing atrophy	Mod. RCD	Mod. Unclear Progression (50)	No	No	c.1004C>T, p.Thr335Met; c.1326delG, p.Ser443Alafs*12
ARSG-29692	F	40	69	20/1000; 20/800	N/A	N/A	Reduced PV and nyctalopia	Yes	Atrophy	N/A	Sev. Stable (50)	Yes	Yes	c.337G>A, p.Gly113Ser; c.337G>A, p.Gly113Ser
ABHD12														
AHBD12–1	F	18	48	20/25; 20/25	N/A	N/A	Nyctalopia	Yes	Atrophy	UD	No	No	No	c.1054C>T, p.Arg352*; c.1196del, p.(*399Serfs*122)
AHBD12–2	F	20	23	20/200; 20/30	28	20/160; 20/160	Nyctalopia	No	Atrophy	Sev. RD, Mild CD	No	No	No	c.1063C>T, p.Arg355*; c.259C>A, p.Pro87Thr
AHBD12–3	M	16	17	20/80; 20/60	22	20/240; 20/240	Blurred CV	No	Bullseye	Mild RCD	No	No	Yes	c.193C>T, p.Arg65*; c.193C>T, p.Arg65*
AHBD12–4	M	22	27	20/300; 20/600	34	20/400; 20/400	Blurred CV, Nyctalopia	Yes	Atrophy	Mod. RD, Mild CD	Mod. Progressive (20)	No	No	c.620–2A>G, Intron 6; c.620–2A>G, Intron 6
AHBD12–5	M	Early 30s	42	CF; CF	53	HM; HM	Blurred CV	Yes	Hole	N/A	Mod. Progressive (44)	No	Yes	c.374C>T, p.Thr125Met; c.1154T>C, p.Leu385Pro
AHBD12–6	M	18	53	LP; LP	N/A	N/A	Blurred CV	No	Atrophy	N/A	Sev. Progressive (20)	No	No	c.784C>T, p.Arg262*; c.867+5G >A, Intron 9

* indicates members of the same family

Author Manuscript Author Manuscript Author Manuscript Author Manuscript

Abbreviations: F, female; M, male; Sx, symptoms; OD, right eye; OS, left eye; BCVA, best corrected visual acuity; PV, peripheral vision; CV, central vision, ICD, impaired color discrimination; VA, visual acuity; CF, count fingers; LP, light perception; HM, hand motion; RPE, retinal pigmented epithelium; ERM, epiretinal membrane; ffERG, full-field electroretinogram; RCD, rod-cone dystrophy; CD, cone dysfunction; RD, rod dysfunction; CRD, cone-rod dystrophy; UD, undetectable; Mod., moderate; Sev., severe; SNHL, sensorineural hearing loss; Ves., vestibular; CS, consanguinity;.